Identification and optimization of a new series of anti-tubercular quinazolinones

Cédric Couturier, Christine Lair, Alain Pellet, Anna Upton, Takushi Kaneko, Corinne Perron, Eric Cogo, Jérome Menegotto, Armin Bauer, Bodo Scheiper, Sophie Lagrange, Eric Bacqué

PII: S0960-894X(16)30983-0
DOI: http://dx.doi.org/10.1016/j.bmcl.2016.09.043
Reference: BMCL 24267

To appear in: *Bioorganic & Medicinal Chemistry Letters*

Received Date: 19 July 2016
Revised Date: 14 September 2016
Accepted Date: 15 September 2016

Please cite this article as: Couturier, C., Lair, C., Pellet, A., Upton, A., Kaneko, T., Perron, C., Cogo, E., Menegotto, J., Bauer, A., Scheiper, B., Lagrange, S., Bacqué, E., Identification and optimization of a new series of anti-tubercular quinazolinones, *Bioorganic & Medicinal Chemistry Letters* (2016), doi: http://dx.doi.org/10.1016/j.bmcl.2016.09.043

Bioorganic & Medicinal Chemistry Letters
journal homepage: www.elsevier.com

Identification and optimization of a new series of anti-tubercular quinazolinones

Cédric Couturier[a]*, Christine Lair[a]; Alain Pellet[a], Anna Upton[b], Takushi Kaneko[b], Corinne Perron[c], Eric Cogo[c], Jérome Menegotto[c], Armin Bauer[d], Bodo Scheiper[d], Sophie Lagrange[a] and Eric Bacqué[a]

[a] *Sanofi R&D, TSU Infectious Disease, 1541, Avenue Marcel Merieux, 69280 Marcy l'Etoile, France.*
[b] *Global Alliance for TB Drug Development, New York, New York 10005, United States*
[c] *Sanofi R&D, Lead Generation and Candidate Realization 195, route d'Espagne BP 13669 31036 Toulouse Cedex 1, France*
[d] *Sanofi Deutschland GmbH, Lead Generation and Candidate Realization, Industriepark Hoechst, 65926 Frankfurt am Main, Germany*

ARTICLE INFO

Article history:
Received
Revised
Accepted
Available online

Keywords:
Tuberculosis
High throughput screening
Antitubercular drugs
Lead opitmization

ABSTRACT

A high throughput phenotypic screening against *M. smegmatis* led us to the discovery of a new class of bacteriostatic, highly hydrophobic antitubercular quinazolinones that potently inhibited the *in vitro* growth of either extracellular or intramacrophagic *M. tuberculosis (Mtb)*, via modulation of an unidentified but yet novel target. Optimization of the initial hit compound culminated in the identification of potent but poorly soluble *Mtb* growth inhibitors, three of which were progressed to *in vivo* efficacy studies. Despite nanomolar *in vitro* potency and attractive PK properties, none of these compounds was convincingly potent in our *in vivo* mouse tuberculosis models. This lack of efficacy may be linked to the poor drug-likeness of the test molecules and/or to the properties of the target.

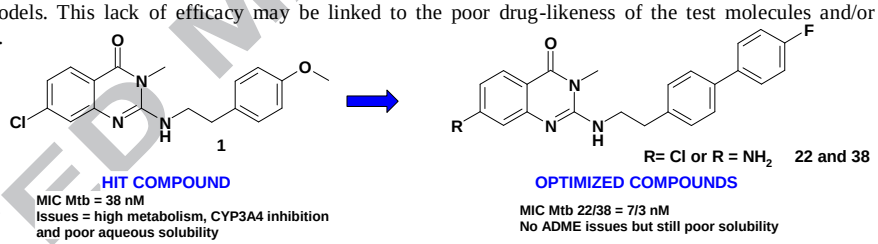

Tuberculosis (TB) is an airborne infectious disease caused by the bacterium *Mycobacterium tuberculosis* (*Mtb*) and that mostly affects the lungs. It is a complex disease caused by different bacterial populations that are located within the host either intracellularly in macrophages or extracellularly within cavities or hypoxic lesions. TB represents one of the top public health concerns worldwide. One-third of the world's population is infected with *Mtb* causing an estimated 9 million new cases and 1.5 million deaths in 2013.[1] The multidrug treatment established in the 1970s and still recommended today by the World Health Organization (WHO) has not been sufficient to eliminate TB due to the advent of HIV/AIDS, failure of treatment programs and emergence of drug-resistant TB[2]. In addition, poor compliance and deficient health care systems have often resulted in treatment interruptions, thereby causing or exacerbating the emergence and spread of drug resistance[2]. The currently recommended combination therapy for drug-sensitive TB is lengthy and complex: 2 months, associating Rifampicin, Isoniazid, Pyrazinamide and Ethambutol, followed by 4 months with Rifampicin and Isoniazid[2]. In the case of multi- and extensive-drug resistant (MDR/XDR) TB, treatments may even require daily medication by multiple and unsafe drugs, for up to 24 months[2].As a consequence, there is an urgent need for the discovery and development of new antitubercular agents that would act by new mechanisms of action and hence would be able to treat both the drug-sensitive and the resistant forms of the disease. With this objective, several paths in the TB drug discovery field have been followed in recent years such as preparing new analogues of TB drugs[3], revisiting the targets of known anti-TB compounds[4], repositioning non-TB drugs[5], tapping into the natural product pool[6], harnessing target-based approaches[7] and conducting traditional growth inhibition screenings[8].

However, for various reasons, most of these strategies have so far met with limited success, with the notable exception of high-throughput (HTS) growth inhibition screenings of small-molecule libraries against *Mtb* (or more frequently against *Mtb* surrogates such as *M. smegmatis* or *M. bovis*). Indeed, this latter approach has delivered in recent years a variety of new anti-TB scaffolds[9]. Along these lines, we conducted a few years ago such a whole cell-based HTS, testing the Sanofi chemical library (800K) against *M. smegmatis*.

* Corresponding authors. Tel.: +33(0)4.37.37.07.35; email cedric.couturier@sanofi.com (C.C.).

Following the screening step at 10µM, dose-responses of compounds inhibiting more than 50% of the bacterial growth were determined. Compounds displaying MIC < 20 µM were then screened against *M. tuberculosis* H37Rv. Confirmed actives were counter-screened vs the human HepG2 cells to discard compounds with unspecific antimycobacterial activities: only compounds with a selectivity index (SI=TC_{50}/MIC) > 10 were selected for further analysis. Sorting and prioritization of the resulting selective actives led to several series, of which quinazolinone **1** emerged as a potential attractive starting point due to its high potency (MIC = 38 nM against H37Rv *Mtb*), an attractive SI (TC_{50} HepG2 = 13.4 µM), good activity against the growth of *Mtb* in mouse macrophages (MIC = 163 nM) and promising activity against drug-resistant *Mtb*. Indeed, when tested on *Mtb* strains mono-resistant to known TB drugs, no-cross-resistance was seen, suggesting a new mechanism of action. Compound **1** was also shown to exhibit bacteriostatic properties against *Mtb* while antimycobacterial potency significantly decreased in the presence of mouse, fetal calf or human sera (for instance MIC shifted from 13 to 429 nM in the presence of 25% mouse serum) suggestive of high protein binding, consistent with high hydrophobicity (see below).

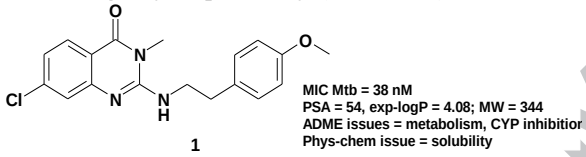

1

Figure 1: Hit Quinazolinone 1

There was no report (in the literature) of anti-Mtb activity or anti-bacterial activity on the analogues of compound **1** which exhibited a high experimental logP (logP = 4.08), significantly different from the calculated value provided by the ACD9 software (clogP = 3). In line with this high logP value, equilibrium aqueous solubility was found to be low at pH 7.4 or 1 (respectively <1 and 11 µg/ml). High hydrophobicity, low polarity (PSA = 54) and the polyaromatic nature of compound **1** all pointed to poor overall drug-like properties, somewhat compensated by a low molecular weight (MW=344). ADMET profiling showed that compound **1** had strong potential for oral absorption as suggested by its high permeability though Caco2 cells (data not shown), moderately inhibited the hERG channel (35% inhibition at 10 µM in an automatic patch clamp assay, at 20°C) and was Ames-negative. Furthermore, while being a weak inductor of CYP3A4, **1** potently inhibited cytochrome CYP3A4 (IC_{50} < 1 µM for the testosterone probe) and also displayed high metabolism in the presence of mouse microsomes, incompatible with *in vivo* efficacy in mouse models of TB. Metabolism was also found high in the presence of human microsomes (see table 4) or human hepatocytes (data not shown). Demethylation of the methoxy group and hydroxylations of the distal aryl ring were identified as the main metabolism pathways.

At this point, we decided to embark on a program aimed at exploring structure-activity relationship around compound **1** while striving to solve the issues identified during the profiling phase, namely high metabolism, CYP inhibition, poor solubility and strong serum shifts. Herein, we report the results of this optimization program that led us to advanced analogues that were tested in mouse infection models. We will discuss the *in vitro* activities as well as the ADMET and drug-like properties across the series. We will also present the *in vivo* antitubercular activities of the best analogues and comment on the reasons for their lack of efficacy.

Synthesis of compounds **1-45** followed the routes described in scheme 1. Three different routes (A, B and C) were used in order to synthesize the targeted compounds. The main difference between these different routes was the nature of the leaving group (thiomethyl or chloro) in intermediates **47** and **50** that was designed to allow the installation of the amino side chain by aromatic nucleophilic substitution. Starting from variously substituted 2-aminobenzoic acids, the thioethers **47** were obtained in two steps following cyclisation with methylthioisocyanate and subsequent methylation of the thiono sulfur atom of **46**. Intermediates **46** were alternatively transformed into compounds **50** upon reaction with sulfuryl chloride. In the cases of substituents such as methoxy or nitro on the aryl ring, compounds **49** were obtained in a three-step sequence from 2-amino benzoic acids: conversion into 2-amino N-methyl amino benzamides **48,** cyclisation into compounds **49** in the presence of carbonyl di-imidazole and treatment with phosphoryl chloride. The targeted compounds **1-45** were finally obtained by condensation of compounds **47** or **50** with various primary amines **51**. In pathway A, intermediates **46** were heated at 160°C with di-isopropyl ethyl amine as the base, in N-methyl pyrrolidinone, to afford compounds **1-8** and **12-45**. Of note, these conditions sometimes proved too drastic, resulting in the degradation of the reaction mixtures and in side products. In these cases, pathways B and C were favored though the chloro intermediates **50** turned out to be quite unstable. Consequently, these intermediates were not stored but rather used directly in the last condensation step. In general, microwave heating of compounds **50** and **51**, in the presence of triethylamine in methanol, during 30 minutes at 130°C, delivered compounds **9-11** in satisfactory yields (40-60 %).

We started our exploration program by investigating the impact on the activity of the length of the ethyl linker between the quinazolinone ring and the distal aromatic ring. A methylene and a propyl chain resulted in a 3-log reduction of activity (see compounds **2** and **3** in table 1), suggesting that the ethyl chain was optimal for activity. Keeping this ethyl chain constant, we then moved our attention toward the N-alkylation pattern of compound **1**. We found that the N-alkylation of compound **1** was optimal: demethylation of the quinazolinone ring nitrogen and methylation of the side nitrogen led to inactive compounds (see **4** and **5**). Likewise, extending the ring N-Me group into N-Et resulted in a very significant drop of activity (see **6**). Regarding the substituents on the quinazolinone moiety (see compounds **7-15** in table 1), the 7-chloro (as in compound **1**) and 7-methyl (see compound **9**) substituents were found to be optimal.

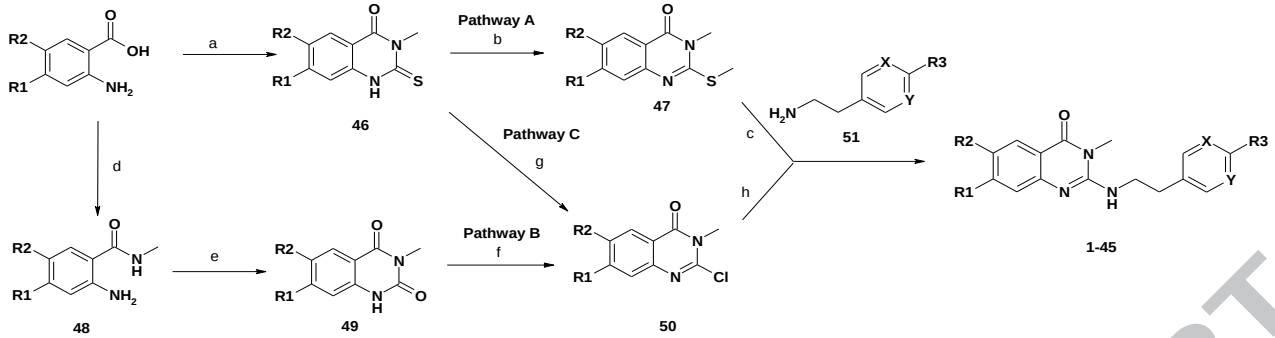

Scheme 1: (a) MeNCS, AcOH, 150°C, 24h (b) Me_2SO_4, NaOH, MeOH, rt, 5h (c) DIEA, NMP, 160°C, 24h (d) $MeNH_2$.HCl, HOBt, DCI, DIEA, DMF, rt, 16h (e) Im_2CO, DBU, THF, rt, 20h (f) $POCl_3$, DIEA, 90°C; 20h (g) SO_2Cl_2, $CHCl_3$, 60°C, 6h (h) Et_3N, EtOH µW, 130°C, 30 min

The other 7-substituted analogues were less active than **1** or even inactive (see the hydrogeno, fluoro, methoxy, cyano, amino and dimethylamino analogues **7-13**). Shifting the chloro atom of compound 1 from position 7 to position 6 yielded compound **14** that was much less active than **1**. Introduction of a nitrogen atom at various positions of the benzo ring of compound **4** proved to be deleterious to potency as well (data not shown). Fluorination of position 6 of the quinazolinone ring of compound **1** was well tolerated and delivered a compound of similar activity as **1** (see compound **15**).

Across this first series of compounds, the serum shifts were generally above ten (data not shown) with the exception of **12** for which the shift was around 5 (MIC : 198 vs 43 nM). These results were in line with the logPs: above 2 or even 3 for all analogues except for **12**. As for **1**, cytotoxicity on HepG2 cells was generally moderate, typically between 10 -> 30 µM: this was not considered a problem for this series considering the high potencies vs *Mtb*. At this point, we focused on the distal aromatic ring. We rapidly discovered that there was little room here to reduce the hydrophobicity of **1**. Substituting the p-methoxy group by a hydrogeno atom (see compound **16** in table 2) or by a more polar moiety (compounds **17** and **18**) resulted in a substantial loss of activity and no gain in terms of serum shifts.

Substituting the distal phenyl ring of **1** for a 2-pyridyl ring (compound **19**) yielded a similar result. On the other hand, whereas a p-OCF_3 group resulted in a less potent compound (**20**), increasing further hydrophobicity by exchanging the methoxy group for an aromatic ring generally resulted in compounds (see compounds **21-23**) with similar or even better potency vs *Mtb* than **1**, in a way that was reminiscent of the optimization of PA-824[10].

Since these biaryl derivatives turned out to possess improved ADMET profiles (see below), we tried to improve the drug-like properties of these derivatives. Introduction of nitrogen(s) on the new terminal aromatic ring was detrimental to activity ring activity (compare **23** with **27** and **28** or **22** with **25** and **30**), unless substituted by a hydrophobic group (compare respectively **24** with **25-28**, **29** with **30-31** and **33** with **34**). We also attempted to disrupt the biaryl moiety by introducing a hydrophobic 4-chloro phenoxy moiety instead of the methoxy group of compound **1**. The corresponding compound **35** proved to retain similar activity compared to **1**. Adding a nitrogen on the aryloxy moiety of compound **34** was tolerated (compound **36**) but removing the chloro atom led clearly, as expected on previous observations, to a less potent compound (see **37**).

Cpd #	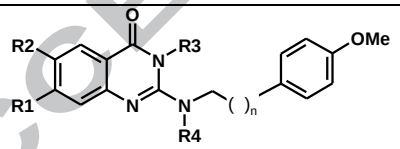					experimental (e) or calculated (c) LogP	MIC* *Mtb* (µM)	IC_{50} HepG2 (µM)
	R1	R2	R3	R4	S			
1	Cl	H	Me	H	1	4.08 (e)/3 (c)	0.04	13.4
2	Cl	H	Me	H	0	2.6 (c)	19.90	15.7
3	Cl	H	Me	H	2	3.4 (c)	5.80	16.8
4	Cl	H	H	H	1	3.2 (c)	6.30	ND
5	Cl	H	Me	Me	1	3 (c)	11.20	>30
6	Cl	H	Et	H	1	3.5 (c)	1.10	21.0
7	H	H	Me	H	1	2.4 (c)	0.24	>30
8	F	H	Me	H	1	2.5 (c)	0.20	>30
9	Me	H	Me	H	1	2.9 (c)	0.01	>30
10	OMe	H	Me	H	1	3.1 (e)/2.3 (c)	0.03	>30
11	CN	H	Me	H	1	1.8 (c)	0.48	12.7
12	NH_2	H	Me	H	1	1.94 (e)/ 1.1 (c)	0.04	ND
13	NMe_2	H	Me	H	1	1.94 (e)/2.5 (c)	0.11	ND
14	H	Cl	Me	H	1	3.2 (c)	0.90	26.1
15	Cl	F	Me	H	1	3.4 (c)	0.03	>30

Table 1: Structure Activity Relationships on the quinazolinone ring and the linker moiety
* MIC determined either by the BactTiter glow method (measure of intracellular ATP by luminescence)

Cpd #	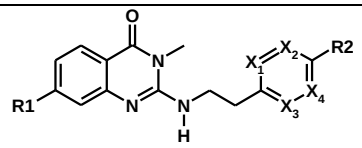				experimental (e) or calculated (c) LogP	MIC* *Mtb* (μM)	MIC* *Mtb* + 25% human-serum (μM)	IC_{50} HepG2 (μM)
	R1	R2	X1	X2				
1	Cl	OMe	CH	CH	4.08 (e)/3(c)	0.04	0.43	13.4
16	Cl	H	CH	CH	4.24 (e)/3.1 (c)	0.06	2.79	15.2
17	Cl	OCH_2CH_2OMe	CH	CH	3.86 (e)/2.7 (c)	0.08	>10	>30
18	Cl		CH	CH	2.2 (c)	0.33	>10	>30
19	Cl	OMe	N	CH	3.32 (e)/2.2 (c)	0.53	ND	27.0
20	Cl	OCF_3	CH	CH	4.95 (e)/4 (c)	0.07	2.33	9.9
21	Cl		CH	CH	5.27 (e)/4.8 (c)	0.01	0.87	6.5
22	Cl		CH	CH	5.28 (e)/4.8 (c)	0.01	0.29	22.0
23	Cl		CH	CH	5.13 (e)/3.3 (c)	0.01	1.47	>30
24	Cl		CH	CH	4.06 (e)/3.5 (c)	0.03	25.16	16.5
25	Cl		CH	CH	4.5 (e)/3.4 (c)	0.02	3.14	19.0
26	Cl		CH	CH	5.04 (e)/4.3 (c)	0.01	0.25	>30
27	Cl		CH	CH	4.67 (e)/3.7 (c)	0.06	ND	11.9
28	Cl		CH	CH	4.68 (e)/4 (c)	0.09	ND	11.3
29	Cl		CH	CH	3.83 (e)/3.2 (c)	0.08	4.06	25.4
30	Cl		CH	CH	4.46 (e)/3.2 (c)	0.01	0.39	>30
31	Cl		CH	CH	5.02 (e)/3.8 (c)	0.02	0.11	>30
32	Cl		CH	CH	4.18 (e)/3.1 (c)	0.02	3.52	>30
33	Cl		CH	CH	3.85 (e)/3 (c)	0.02	8.56	17.3
34	Cl		CH	CH	4.67 (e)/3.9 (c)	0.01	0.86	21.6
35	Cl		CH	CH	5.66 (e)/5.7 (c)	0.04	1.90	10.9
36	Cl		CH	CH	4.94 (e)/4.1 (c)	0.02	1.76	13.0
37	Cl		CH	CH	3.3 (c)	0.06	7.37	12.1
38	NH_2		CH	CH	3.3 (e)/2.9 (c)	0.01	0.01	>30
39	Cl		N	CH	3.5 (c)	0.68	ND	18.3
40	Cl		N	CH	4.23 (e)/3.4 (c)	0.06	4.02	13.9
41	Cl		N	CH	4.03 (e)/3.3 (c)	0.32	ND	14.7
42	Cl		N	CH	2.7 (c)	0.31	>15	24.1
43	Cl		N	N	3.2 (c)	1.12	ND	15.1
44	Cl		N	N	4.67 (e)/3.9 (c)	0.03	3.32	>30
45	Cl		N	N	3.3 (c)	0.74	ND	ND

Table 2: Structure Activity Relationships on the distal aromatic ring

* MIC determined either by the BactTiter glow method (measure by luminescence of intracellular ATP).

In a new effort to conciliate high potency and lower logP in the bi-aryl sub-series, we combined the anilino moiety of compound **12** (the compound from the first series with the best compromise potency/logP) with the p-fluorophenyl of compound **22** (the most potent compound of the series). We were delighted to find that the resulting compound **38** retained nanomolar potency. Finally, in a last effort to decrease the logP of the biaryl analogues, we tried to introduce nitrogen atoms on the first phenyl moiety. As observed for compound **19**, this extra polarity systematically resulted in less potent compounds (**39** to **45**) as well as no gain in serum shift (when measured).

For compounds **16** to **45**, serum shifts ranged from 8 (for compound **19**) to ~200 for compound **23**. The highest shifts were generally associated to the most potent biaryl derivatives, thereby totally obliterating the benefit of the high potencies observed without serum (see for example, compounds **22** and **23**). The few exceptions to this rule were for the more polar, less hydrophobic, compounds such as **26**, **30, 31** and **38**. In the latter case, the serum effect was still important (~30; comparable to **1)** but deemed as acceptable considering the level of remaining potency (MIC with serum = 84 nM). As previously noted, cytotoxicity remained moderate to weak across this new set of compounds (typically in the 10 to > 30µM range).

We also looked at the capacity of our best compounds to inhibit growth inhibition of *Mtb* in macrophages, a known compartment of *Mtb* in humans[11]. Against mouse macrophages, activities were consistently good (generally below the 200 nM bar) across the series (see table 3) and generally well correlated with MICs vs extracellular *Mtb*, with a few exceptions. The ratios between the two types of MICs were typically between 1 and 10 and ranged from 0.6 (for **30**) to almost 160 (for **31**), without clear structural rationale (compare **25**, **30**, **32** and **40** with **22** and **31**). Hydrophobicity didn't seem to play a role here as demonstrated by the comparisons between the less hydrophobic **1** and **38** with the highly hydrophobic **22** and **35** that all yielded similar good intramacrophagic activities (MICs = from 60 to 163 nM).

In parallel to this SAR exploration exercise, we profiled our best quinazolinones in a series of ADMET and physico-chemical assays. We first checked that, across the series, Caco2 permeability and hERG inhibition were generally acceptable (data not shown). Then, we investigated the impact of structural variations on the main issues of the hit compound, namely aqueous solubility, metabolism and CYP3A4 inhibition (see table 4). Replacement of the chloro substituent on the quinazolinone ring of **1** generally resulted in increased metabolism in microsomes and only slight improvements in solubility at pH1 (see compounds **9** and **10** in table 3).Simple variations on the distal aromatic ring didn't improve metabolic stability but occasionally improved solubility when polarity was introduced (see **16**, **18** and **19**).

In contrast, substituting the para-MeO group on the distal aromatic ring of **1** by a phenyl or a trifluoromethoxy moiety clearly dampened metabolism though at the expense of solubility (see **20**, **21** and **22**). Addition of nuclear nitrogens on either ring of the biaryl moiety did significantly improve solubility while retaining good metabolic stability (see **24**, **29** and **33**) but these gains in solubility were rapidly lost upon attachment of the kind of hydrophobic groups that provided high antimycobacterial potency (see **23**, **25**, **26**, **30**, **31, 32** and **34**). Likewise, attachment at the para position of the distal aromatic of a chloro-substituted (hetero)aryloxy moiety resulted in insoluble compounds with high metabolic stability (see **35** and **36**). Compound **38** that combined a p-fluoro biaryl moiety with a polar 7-amino quinazoline moiety displayed slightly better solubility compared to **22** and moderate metabolism.

Cpd #	Structure	MIC (nM) without serum	MIC (nM) mouse macrophage
1	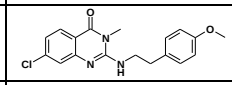	38	163
21	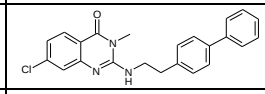	8	164
22	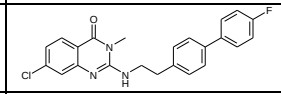	3	60
25	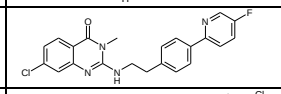	15	51
26	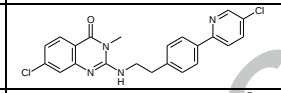	2	63
30	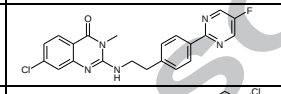	3	13
31	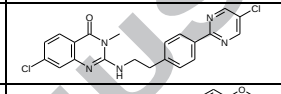	6	947
32	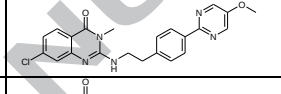	16	81
35	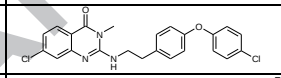	36	133
38	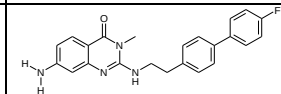	4	60
40	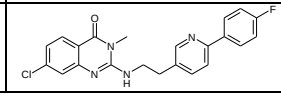	57	201

Table 3: Best compounds in mouse macrophages infected by *Mtb*

Regarding CYP3A4 inhibition, the 2-mono-aryl ethyl amino derivatives (compounds **2** to **20**) generally retained potent inhibition (for example, see in table 4, compounds **9**, **10** and **19**) with a few exceptions such as **16** and a few para-substituted aryl derivatives (see for representative examples, **18** and **20**) where inhibition was more moderate. Along similar lines, the biaryl derivatives turned out to be weak to moderate inhibitors of CYP3A4 (eg **21**, **22**, **25**, **26**, **30**, **31** and **38**) though the improvement was less marked for the least hydrophobic analogues (see for instance **23**, **24**, **29** and **32**). Biaryloxy derivatives behaved similarly (see **35** and **36**).

At the end of this exploration/optimization phase, it was clear that we had been unable to find an acceptable compromise between high potency, moderate hydrophobicity and good ADMET profile. Compound **38** turned out to be the best balance we could reach: it displayed potent antimycobacterial activities (with and without serum), with high caco2 permeability, limited metabolism (only 33% of which was mediated by CYP3A4) and weak inhibition of CYP3A4 as well as of the hERG channel (22% inhibition at 10µM), even if its aqueous solubility was quite low.

Overall, we concluded that parallel optimization of the ADMET properties and of the potency against *Mtb* had led us into an unfavorable corner of the physico-chemical space, an analysis already formulated by others[8b,8c].

Cpd #	Structure	MIC (nM) without serum	Solubility[a] pH1/7.4 (µg/ml)	% of metabolic lability (h/m/r)[b]	CYP3A4 IC_{50} (T/M)[c] (µM)
1	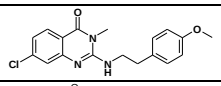	38	157/1	51/68/18.5	4.3 / <1
9	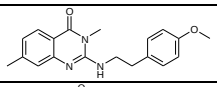	11	221/<1	89/99/97	4.8 / <1
10	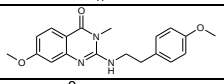	26	734/4	90/86/52	10 / <1
16	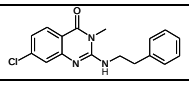	62	180/<1	65/66/27	18 / 11
18	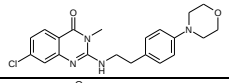	332	1091/8	58/12/40	11 / 11
19	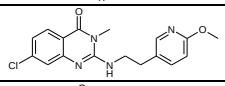	532	1138/9	41/47/17	7.4 / <1
20	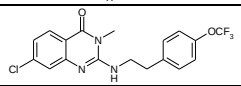	70	43/<1	9/32/0	>30 / 4
21	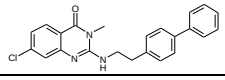	8	5/<1	18/21/26	>30 / >30
22	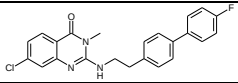	3	<1/<1	0/7/11	18 / >30
23	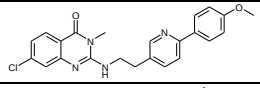	7	26/<1	28/0/23	7.9 / 8
24	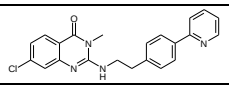	27	1107/<1	17/10/26	5.8 / 15
25	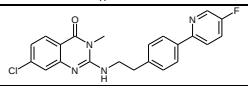	15	44/<1	0/16/15	9.3 / 41
26	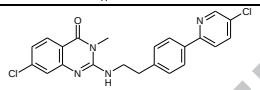	2	21/<1	3/9/20	8.4 / >30
29	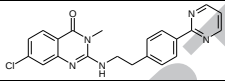	79	246/<1	3/6/28	5.4 / 13
30	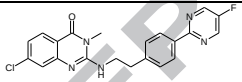	3	11/<1	0/0/1	9.9 / >30
31	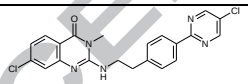	6	10/<1	7/12/18	16 / >30
32	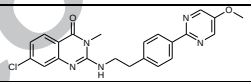	16	37/<1	14/0/15	8.7 / 11
33	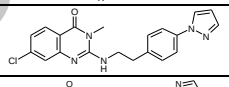	61	138/<1	19/27/35	8.3 / 27
34	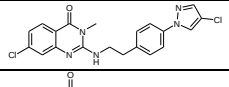	12	<1/<1	0/1/5	- / 16
35	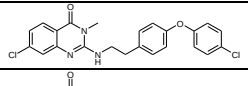	36	<1/<1	17/3/9	29 / 14
36	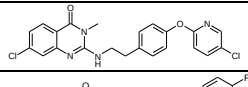	23	<1/<1	10/6/3	15 / 9.8
38	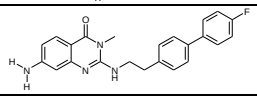	4	13/<1	10/27/19	30 / 23

Table 4: Structure Property Relationship of selected quinazolinones

a: Equilibrium solubility at 20°C; b: % of metabolized compound (initial concentration: 5µM) after 20' incubation, in the presence of 1 mg/mL of human/mouse or rat of microsomal proteins and of 1 mM of NADPH; c: testosterone (T) or midazolam (M) probes

At this point, we were ready to assess the *in vivo* efficacy of our best derivatives in mouse model of highly acute tuberculosis infection. We started with compound **35**, a typical representative of the series with high *in vitro* potency (MIC = 36 nM), a serum effect was noted (MIC = 420/2100 nM in the presence of 25% of mouse/human serum), in line with high protein binding in humans and mouse (99.9%), good intramacrophagic activity (MIC = 133 nM) and poor aqueous solubility (< 1 µg/ml at pH 7). Mouse PK of **35** indicated good oral bioavailability (90%, iv 3 mg/kg) as a solution in NMP / Solutol HS15 / PBS pH7.4 (5%/5%/90%) formulation. Similar exposures were obtained using a Vitamin E TPGS /Water (50%/50%) or a Lipidic vehicle (Cremophor RH40/Capryol 90/Miglyol 812N (10%/20%/70%) half diluted in water (Pre-emulsified formulation). The VitE formulation was first used for *in vivo* activity evaluation. A lack of potency at the higher tested dose was observed and in order to improve exposure, we used the Pre-emulsified (Lipidic/Water) formulation for the 600 mg/kg dose. In this formulation, plasma AUCs were dose-proportional between 10 and 100 mg/kg (21 to 290 µg.h/ml) and at 100 mg/kg, plasma and lung concentrations remained above the MIC value in the presence of mouse serum for more than 96 hours. Despite these encouraging PK properties, when tested in our TB infection model, compound **35** showed only weak efficacy: the Minimum Effective Dose (MED) was only approached at 600 mg/kg (see Figure 2).

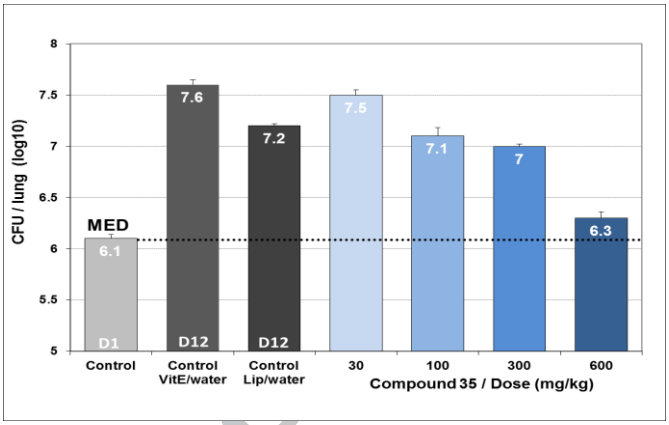

Figure 2: ***In vivo*** **mouse model of acute TB with compound 35: mice were infected by H37Rv strain day 1 (D1).A daily oral gavage started D2 for 2 weeks (4 days by week). Compound is formulated in VitE/water or in Lipidic/water (for 600 mg/kg) and controls received the vehicle alone. Efficacy was assessed at D12 by the decline in lung CFU counts.**

Looking for a compound that would retain more potency than **35** in the presence of serum, we then turned our attention to compound **22**. Since its MIC was 3 nM on replicating *Mtb* following 5 days incubation and 34/250nM with 25% of mouse/human serum. It was also highly active intra-macrophages (MIC = 60 nM). Aqueous solubility of this compound was low (< 1 µg/ml at pH 7); a new PEG200/Vitamin E TPGS (90%/10%) formulation allowed reasonable solubility (20 mg/ml) and exposures in mice. In this formulation, oral bioavailability in mice was 73% and plasma exposure reached 76 µg.h/ml at 100 mg/kg *po*. Lung tropism was good (lung / plasma ratio= 14) and half-life in plasma was long (8 h). Furthermore, time over the MIC in the presence of mice serum was above 24 hours in both plasma and lungs. Of note, higher doses than 100 or 200 mg/kg failed to significantly improve exposures due to solubility limitations. When tested in the highly acute model at doses ranging from 12.5 to 200 mg/kg, compound **22** showed a very disappointing flat *in vivo* response (see figure 3) in line also with high protein binding in humans and mouse (99.9%).

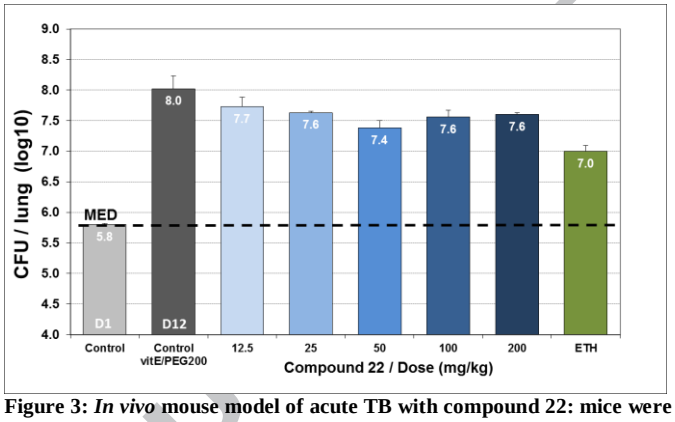

Figure 3: ***In vivo*** **mouse model of acute TB with compound 22: mice were infected by H37Rv strain day 1 (D1).A daily oral gavage started D2 for 2 weeks (4 days by week). Compound is formulated in VitE TPGS/PEG 200 (10%/90%) and compared to Ethambutol (ETH)). Controls received vehicle alone. Efficacy was assessed at D12 by the decline in lung CFU counts.**

As poor solubility was hypothesized to be a limiting factor in the GI tract due to potential risk of re-precipitation anticipated with co-solvent/surfactant formulation, we decided to switch to an alternative formulation strategy identifying a sulfate salt of **22** that could be formulated in a 5% Soluplus/Acetate buffer formulation between 10 to 300 mg/kg. In this formulation, plasma concentrations at 300 mg/kg were above the MIC with serum for more than 24 hours (AUC: 140 µg.h/ml at 300 mg/kg *po)* and lung exposure was clearly improved (AUC at 300mg/kg: 980 µg.h/ml versus 55 in VitE/PEG200).

In the highly acute model, each 4 days dosing are separated by a 2 days washout. Taking into account the bacteriostatic effect of the series, we decided to modify the model by treating mouse daily for 8 continuous days. Following 8 consecutive daily doses, compound **22** demonstrated MED at 300 mg/kg (see figure 4). However, efficacy was not confirmed when 2*4 day dosing periods were separated by 2 days without treatment (0.78 log reduction versus 1.5 log without dosing break). Due to the large discrepancy between *in vitro* activity and the poor *in vivo* activity obtained in our efficacy studies, despite good *in vivo* exposures, we decided to stop with this compound.

Finally, we selected compound **38**, the compound that had emerged from the optimization phase as displaying the best balance between potency (MIC= 4nM; MIC with human/mice serum= 84/7 nM; intramacrophagic MIC = 60 nM) and hydrophobicity (solubility at pH 1 = 13 µg/ml; high protein binding in humans and mouse (99.8%).). Though PK properties at 100 mg/kg (mice; formulation VitE/PEG200/HPC (19%/79%/2%); *po*) looked in first analysis less attractive than those of **22** and **35** (AUC = 29 µg.h/ml; $t_{1/2}$≈ 6h, lung/plasma ratio = 4.5), we nevertheless decided to assess the *in vivo* efficacy of **38**

hoping that improved *in vitro* potency in the presence of serum would compensate for diminished exposures.

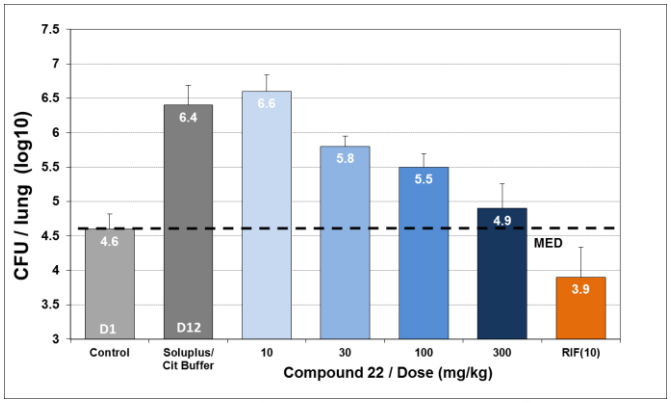

Figure 4: ***In vivo*** **mouse model of acute TB with compound 22-sulfate. Mice were infected by H37Rv strain day 1 (D1). A daily oral gavage started D2 for 2 weeks (10 treatment in Soluplus/ acetate buffer formulation) and compared to Rifampycin (RIF) at 10 mg/kg. Efficacy was assessed at D12 by the decline in lung CFU counts.**

This expectation turned out not to be met: against highly acute murine, a flat lung CFU reduction response was observed over the dose range of 10-100 mg/kg (see Figure 5). Furthermore, toxicity after one treatment at 300 mg/kg prevented any increase of doses.

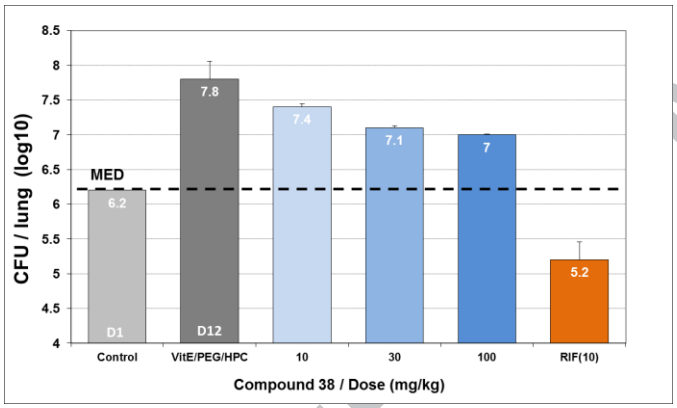

Figure 5: ***In vivo*** **mouse model of acute TB with compound 38 mice were infected by H37Rv strain day 1 (D1).A daily oral gavage started D2 for 2 weeks (4 days by week). Compound is formulated in VitE/PEG200/HPC (19%/79%/2%) and compared to Rifampycin (RIF) at 10 mg/kg. Controls received vehicle alone. Efficacy was assessed at D12 by the decline in lung CFU counts.**

Overall, despite good *in vitro* potencies even in the presence of serum (at least for compounds **22** and **38)**, potent intra macrophage activities and good PK properties (eg time above the MICs in the presence of serum and good exposures in lung), we have failed to demonstrate convincing *in vivo* efficacy for any member of the quinazolinone series. In the best cases, we only came close to the MED at high doses (300 to 600 mg/kg with optimized formulation).

Reasons for this lack of efficacy were not elucidated. We could only speculate that part of the failure was compound-related. Assays trying to generate compound-resistant mutants with this bacteriostatic series, revealed an unexpected profile: MICs were dependent of inoculum concentration, not allowing us to obtain mutants for target identification. MIC on agar medium for compound 22 shifts from 0.016µg/ml to 2µg/ml for 1000 and 100 000 bacteria inoculated respectively on agar plates. In the mouse model of highly acute TB, 1.10^6 bacteria are inoculated to each mouse giving a lung burden from 1.10^6 to 1.10^8 CFU at the end of the experiment. Taking into account the MIC shift, the limited free fraction available and the incapacity to increase doses due to poor solubility, a too low compound concentration available in lungs could explain the poor *in vivo* activity observed. Another key point for *in vivo* activity is the compound distribution in pulmonary lesions[11] which is unknown for this series. Failure could also be target-related due to their bacteriostatic effect[8b, 8c], to a lack of *in vivo* vulnerability[12] or linked to the already reported inherent difficulty to correlate PK properties and *in vivo* efficacy for anti-TB compounds[13].

As frequently observed for anti-tubercular series stemming from phenotypic screenings, we had to face the combined difficulties of not knowing the target (and hence if it is a validated target *in vivo*) and of selecting a non-lead-like hit compound that upon subsequent optimization led us, because of the greasy membrane of *Mtb*, to potent but highly hydrophobic compounds whose properties are unfavorable to allow demonstration of *in vivo* efficacy at reasonable doses[8b, 8c]. Based on these disappointing results and in the absence of evidence that we would be able to improve the drug-like properties of the series upon further optimization, the series was discontinued and we didn't attempt to identify the target.

The quinazolinone series has been identified as a potential new class of anti-tubercular drugs following a growth inhibition HTS against *M. smegmatis* used as a surrogate of *Mtb*. The attractive microbiological profile of the hit compound, including its likely novel (and unidentified) mechanism of action, prompted us to initiate an optimization program aimed at delivering prototype compounds able to rapidly achieve *in vivo* proof of concept in the mouse model of highly acute *Mtb* infection and hence demonstrate the potential of the series to afford a development candidate. Our effort led us to compounds with single-digit nanomolar *in vitro* potency against *Mtb*, moderate serum effect, no CYP liabilities and dampened metabolism. However, the best compounds still displayed high hydrophobicity, low aqueous solubility, non-proportional oral mice PK at high doses and overall poor drug-likeness. Furthermore, we were unable to demonstrate significant *in vivo* efficacy for three analogues, in the highly acute mice tuberculosis infection model. Our work illustrates the difficulties to establish *in vivo* proof of concept for poorly drug-like anti-tubercular hit compounds that usually stem from *Mtb* growth inhibition screening.

On a more positive concluding note, unveiling the unknown target of the quinazolinone series should deliver a novel mycobacterial target, which in case of validation of its *in vivo* interest, may help find, following a new target-based screening, alternative and hopefully more attractive chemical matter than the compounds of this work.

Literature

1. WHO: World Health Organization: Global tuberculosis report 2015. In.; 2015.

2. (a) WHO: World Health Organization: Global MDR-TB situation **2014**. In.; 2014 (b) Dheda, K.; Migliori, G. B. *Lancet* **2012**, 379, 773.
3. (a) Sacksteder, K. A.; Protopopova, M.; Barry C. E. 3rd; Andries, K; Nacy, C. A. *Future Medicine* **2012**, 823 (b) Zhang, D.; Lu, T.; Liu, K.; Liu, B.; Wang, J.; Zhang, G.; Zhang, H.; Liu, Y; Wang, B.; Zheng, M.; Fu, L.; Hou, Y.; Gong, N.; Lv, Y.; Li, C.; Cooper, C. B.; Upton, A. M.; Yin, D.; Ma, Z.; Huang, H. *J. Med. Chem.* **2012**, 55, 8409 (c) Briguglioa, I.; Pirasa, S.; Coronaa, P.; Pirisia, M. A.; Jabesb, D.; Cartaa, A. *Anti-Infective Agents* **2013**, 75, 4. (a) Hameed, S. P.; Manjrekar, P.; Raichurkar, A.; Shinde, V.; Puttur, J.; Shanbhag, G.; Chinnapattu, M.; Patil, V.; Rudrapatana, S.; Sharma, S.; Kumar N. C. N., Nandishaiah, R.; Madhavapeddi, P.; Sriram, D.; Solapure, S.; Sambandamurthy, V. K. *ACS Med. Chem. Lett.* **2015**, 6, 741 (b) Christopher P. Locher, C. P.; Jones, S. V.; Hanzelka, B. L.; Perola, E.; Shoen, C. M.; Cynamon, M. H.; Ngwane, A. H.; Wiid, I. J.; van Helden, P. D.; Betoudji, F.; Nuermberger, E. L.; Thomson, J. A. *Antimicrob. Agents Chemother.* **2015**, 59, 1455 (c) Hartkoorn, R. C.; Sala, C.; Neres, J.; Pojer, J.; Magnet, S.; Mukherjee, R.; Uplekar, S.; Boy-Röttger, S.; Altmann, K.; Cole, S. T. *EMBO Mol Med* **2012**, 4, 1032.
5. (a) Palomino, J. C.; Martin, A.; *J. Antimicrob Chemother* **2012**, 1 (b) Lougheed K. E. A.; Taylor, D. L.; Osborne, S. A.; Bryans, J. S.; Buxton, R. S. **2009**, 89, 364 (c) Ashtekar, D.R.; Costa-Periera, R.: Shrinivasan, T. *Diagn Microbiol. Infect. Dis.* **1991**, 14, 465 (d) Jean-Emmanuel Hugonnet, J.; Tremblay, L. W.; Boshoff, H. I.; Barry, C. E. 3rd; Blanchard, J. S. *Science* **2009**, 1215.
6. (a) Salomon, C. E.; Schmidt, L. E. *Current Topics Med. Chem.* 2012, 12(7), 735 (b) García, A.; Bocanegra-García, V.; Palma-Nicolás, J. P.; Rivera, G. *Eur. J. Med. Chem.* **2012**, 49, 1 (c) Lee, R. E.; Hurdle, J. G.; Liu, J.; Bruhn, D. F.; Matt, T.; Scherman, M. S.;Vaddady, P. K.; Zheng, Z.; Qi, J.; Akbergenov, R.; Das, S.; Madhura, D. B.; Rathi, C.; Trivedi, A.; Villellas, C.; Lee, R. B.; Kesh, R.; Waidyarachchi, S. L.; Sun, D.; McNeil, M. R.; Ainsa, J. A; Boshoff, H. I.; Gonzalez-Juarrero, M.; Meibohm, B.; Böttger, E. C.; Lenaerts, A. J. *Nature Medecine*, **2014**, 152 (d) Nikonenko, B. V.; Reddy, V. M.; Protopopova, M.; Bogatcheva, E.; Einck, E.; Nacy, C. A. *Antimicrob Agents Chemother* **2009**, 53(7), 3138.
7. (a) Kana, B. D.; Karakousis, P. C.; Parish, T.; Dick, T. *Tuberculosis* 2014, 94, 551 (b) Miller, C. H.; O'Toole R. F. *Expert Opin. Drug Discov.* 2011, 6(8), 839 (c) Xiong, X.; Xu, Z.; Yang, Z.; Liu, Y.; Wang, D.; Dong, M; Parker, E. J.; Zhu, W. *Current Drug Targets* **2013**, 14, 676.
8. (a) Cooper, C. B. *J. Med. Chem.* **2013**, 56, 7755 (b) Manjunatha U. H.; Smith, P. W. *Bioorganic Med. Chem.* **2015**, 23, 5087 (c) Jiricek, J. *Future Med. Chem* **2014**, 6 (12), 1377.
9. (a) Ananthan, S., Faaleolea, E. R. , Goldman, R. C.; Hobrath, J. C.; Kwong, C. D.; Laughon, B. E.; Maddry, J. A.; Mehta, A.; Rasmussen, L.; Reynolds, R. C.; Secrist III, J. A.; Shindo, N.; Showe, D. N.; Sosa, M. I.; Suling, I. J.; White E. L. *Tuberculosis*, **2009**, 89, 334 (b) Robert C. Reynolds, R. C.; Ananthan, S.; Faaleolea, E.; Hobrath, J. V.; Kwong, C. D.; Maddox, C.; Rasmussen, L.; Sosa, M.; Thammasuvimol, E.; White, E. L.; Zhang, W.; Secrist, J. A. III *Tuberculosis* **2012**, 92, 72 (c) Kang, S.; Kim, R. Y.; Seo, M. J.; Lee, S.; Kim, Y. M.; Seo, M.; Seo, J. J.; Ko, Y.; Choi, I.; Jang, J.; Nam, J.; Park, S.; Kang, H.; Kim, H. J.; Kim, J.; Ahn, S.; Pethe, K.; Nam, K.; No, Z.; Kim, J. *J. Med. Chem.* **2014**, 57, 5293 (d) Andries, K.; Verhasselt, P.; Guillemont, J.; Gohlmann, H. W.; Neefs, J. M.; Winkler, H.; Van Gestel, J.; Timmerman, P.; Zhu, M.; Lee, E.; Williams, P.; de Chaffoy, D.; Huitric, E.; Hoffner, S.; Cambau, E.; Truffot-Pernot, C.; Lounis, N.; Jarlier, V. *Science* **2005**, 307, 223 (e) Stover, C. K.; Warrener, P.; VanDevanter, D. R.; Sherman, D. R.; Arain, T. M.; Langhorne, M. H.; Anderson, S. W.; Towell, J. A.; Yuan, Y.; McMurray, D. N.; Kreiswirth, B. N.; Barry, C. E.; Baker, W. R. *Nature* **2000**, 405, 962 (f) Makarov, V.; Manina, G.; Mikusova, K.; Möllmann, U.; Ryabova, O.; Saint-Joanis, B.; Dhar, N.; Pasca, M. R.; Buroni, S.; Lucarelli, A. P.; Milano, A.; De Rossi, E.; Belanova, M.; Bobovska, A.; Dianiskova, P.; Kordulakova, J.; Sala, C.; Fullam, E.; Schneider, P.; McKinney, J. D.; Brodin, P.; Christophe, T.; Waddell, S.; Butcher, P.; Albrethsen, J.; Rosenkrands, I.; Brosch, R.; Nandi, V.; Bharath, S.; Gaonkar, S.; Shandil, R. K.; Balasubramanian, V.; Balganesh, T.; Tyagi, S.; Grosset, J.; Riccardi, G.; Cole, S. T. *Science* **2009**, 324, 801 (g) Brown, J. R.; North, E. J.; Hurdle, J. G.; Morisseau, C.; Scarborough, J. S.; Sun, D.; Kordulakova, J.; Scherman, M. S.; Jones, V.; Grzegorzewicz, A. *Bioorg. Med. Chem.* **2011**, 19, 5585.
10. (a) Sutherland, H. S.; Blaser, B., Kmentova, I.; Franzblau, S. G.; Wan, B.; Wang, Y.; Ma, Z; Palmer, B. D.; Denny, W. A.; Thompson, A. M. *J. Med. Chem.* **2010**, 53, 855 (b) Kmentova, I.; Sutherland, H. S.; Palmer, B. D.; Blaser, A.; Franzblau, S. G.; Wan, B.; Wang, Y.; Ma, Z.; Denny, W. A.; Thompson, A. M. *J. Med. Chem.* **2010**, 53, 8421 (c) Blaser, A.; Palmer, B. D.; Sutherland, H. S.; Kmentova, I.; Franzblau, S. G.; Wan, B.; Wang, Y.; Ma, Z.; Thompson, A. M.; Denny, W. A. *J. Med. Chem.*, **2012**, 55, 312 (d) Palmer, B. D.; Sutherland, H. S.; Blaser, A.; Kmentova, I.; Franzblau, S. G.; Wan, B.; Wang, Y.; Ma, Z.; Denny, A. M.; Thompson, A. M. *J. Med. Chem.*, **2015**, 58, 3036.
11. Dartois, V.; Barry, C. E. 3rd *Bioorg. Med. Chem Lett.* **2013**, 23, 4741.
12. Wei, J. R.; Krishnamoorthy, V.; Murphy, K.; Kim, J. H.; Schnappinger, D.; Alber, T.: Sassetti, C. M.; Rhee, K. Y.; Rubin, E. J. *Proc. Natl. Acad. Sci. USA* **2011**, 108:4176e81.
13. Lakshminarayana, S. B.; Huat, T. B.; Ho, P. C.; Manjunatha, U. H.; Dartois, V.; Dick, T.; Srinivasa P. S. Rao, S. P.S. *J. Antimicrob. Chemother.* **2015**, 70, 857.

Supplementary data associated with this article can be found in the online version.

Graphical Abstract

A high throughput phenotypic screening against *M. smegmatis* led us to the discovery of a new class of bacteriostatic, highly hydrophobic antitubercular quinazolinones that potently inhibited the *in vitro* growth of either extracellular or intramacrophagic *M. tuberculosis (Mtb)*, via modulation of an unidentified but yet novel target. Optimization of the initial hit compound culminated in the identification of potent but poorly soluble *Mtb* growth inhibitors, three of which were progressed to *in vivo* efficacy studies. Despite nanomolar *in vitro* potency and attractive PK properties, none of these compounds was convincingly potent in our *in vivo* mouse tuberculosis models. This lack of efficacy may be linked to the poor drug-likeness of the test molecules and/or to the properties of the target.

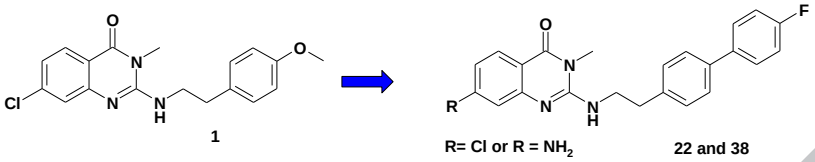

HIT COMPOUND

MIC Mtb = 38 nM
Issues = high metabolism, CYP3A4 inhibition and poor aqueous solubility

OPTIMIZED COMPOUNDS

MIC Mtb 22/38 = 7/3 nM
No ADME issues but still poor solubility